Journal of proteome research

ARTICLE

pubs.acs.org/jpr

Pulsed Stable Isotope Labeling of Amino Acids in Cell Culture Uncovers the Dynamic Interactions between HIV-1 and the Monocyte-Derived Macrophage

Stephanie D. Kraft-Terry,[†] Ian L. Engebretsen,[†] Dhundy K. Bastola,[‡] Howard S. Fox,[†] Pawel Ciborowski,[†] and Howard E. Gendelman[†,*]

[†]Department of Pharmacology and Experimental Neuroscience, University of Nebraska Medical Center, Omaha, Nebraska 68198-5880, United States

[‡]School of Interdisciplinary Informatics, University of Nebraska-Omaha, Omaha, Nebraska 68182-0116, United States

Supporting Information

ABSTRACT: Dynamic interactions between human immunodeficiency virus-1 (HIV-1) and the macrophage govern the tempo of viral dissemination and replication in its human host. HIV-1 affects macrophage phenotype, and the macrophage, in turn, can modulate the viral life cycle. While these processes are linked to host−cell function and survival, the precise intracellular pathways involved are incompletely understood. To elucidate such dynamic virus−cell events, we employed pulsed stable isotope labeling of amino acids in cell culture. Alterations in *de novo* protein synthesis of HIV-1 infected human monocyte-derived macrophages (MDM) were examined after 3, 5, and 7 days of viral infection. Synthesis rates of cellular metabolic, regulatory, and DNA packaging activities were decreased, whereas, those affecting antigen presentation (major histocompatibility complex I and II) and interferon-induced antiviral activities were increased. Interestingly, enrichment of proteins linked to chromatin assembly or disassembly, DNA packaging, and nucleosome assembly were identified that paralleled virus-induced cytopathology and replication. We conclude that HIV-1 regulates a range of host MDM proteins that affect its survival and abilities to contain infection.

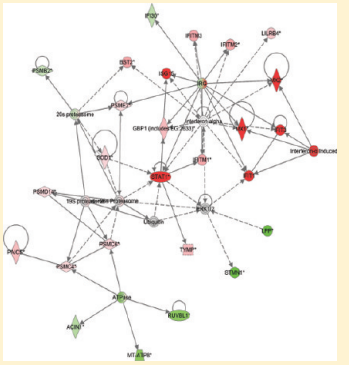

KEYWORDS: monocyte-derived macrophages, human immunodeficiency virus, pulsed stable isotope labeling of amino acids in cell culture, proteome, cell function

INTRODUCTION

Mononuclear phagocytes (MP; monocytes and tissue macrophages) play a prominent role in human immunodeficiency virus (HIV) transmission, viral tissue dissemination, and disease pathogenesis.[1−6] Although MP serve as long-lived viral reservoirs,[2] the biological outcomes of virus-cell interactions are multifaceted and can lead to symbiosis or cell death.[1] For the virus, latency, restriction, or progeny virion production are the final outcomes of cell infection and are closely aligned to cell differentiation and activation.[3] Without a doubt, HIV-1 serves as a conductor for its own regulation, utilizing cross interactions between its own constituents and MP factors.[4] Importantly, while viral infection is modulated through host cell factors, the virus, in turn, influences MP function. The inevitable outcome may change during the viral life cycle and as infection persists.[7] Even after a quarter century of study, how such events occur and what level of MP viral infection influences cytotoxicity remains unclear and poorly defined.

MP protein synthesis can change during differentiation and activation or be cued by the virus itself to either propel or restrict viral growth.[4−6] As per the latter, cell responses to infection ultimately break down and sustain viral growth.[8] The mechanisms by which such activities occur can now be deciphered through the advent of new technologies developed for protein identification and quantification. Sampling and analysis may now be performed at specific times following viral exposure and, as such, could begin to elucidate the biochemical mechanisms operative during the interplay between the virus and its host cell. One means to achieve this goal is through stable isotope labeling of amino acids in cell culture (SILAC). The technique is used commonly to identify differential expression of proteins in studies utilizing cell lines.[9,10] More recently, pulsed SILAC (pSILAC) was developed for quantitation of *de novo* cellular protein synthesis, without the necessity for complete label incorporation.[11] Application of pSILAC is ideal for studying nondividing cells during defined time periods and for quantifying differential protein expression rates.[12] Use of SILAC to assess macrophage infection, activation, and function is new to cell biology since it was introduced only two years ago to study transformed cell lines.[13−17] For the first time, we now report changes in *de novo* protein synthesis for HIV-1-infected primary human monocyte-derived macrophages (MDM) as determined by pSILAC. The identified MDM responses to HIV-1 infection included robust changes in synthesis rates of several protein classes, including those linked to interferon (IFN) signaling and

Received: February 14, 2011
Published: April 18, 2011

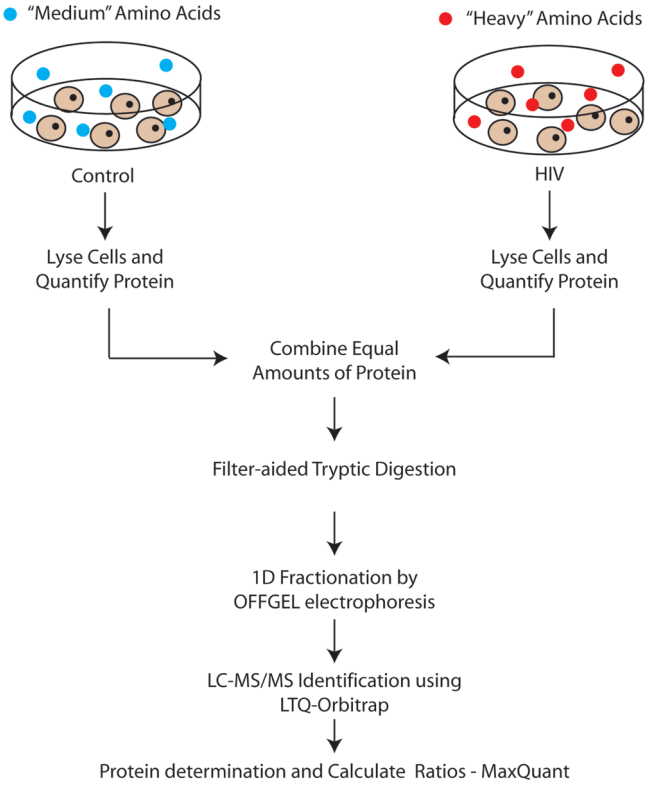

Figure 1. pSILAC experimental design for HIV-1 infection of primary human macrophages. Control cells were treated for 48 h with [$^{13}C_6$]-L-Arginine and [D_4]-L-Lysine, while at the same time, HIV-1-infected cells were treated with [$^{13}C_6$, $^{15}N_4$]-L-Arginine and [$^{13}C_6$, $^{15}N_2$]-L-Lysine. MDM were lysed and protein was quantified. Equal amounts of protein were combined, separated by OFFGEL electrophoresis, sequenced by LC−MS/MS and quantified using MaxQuant.

antigen presentation. The most significant protein groupings were related to cell fusion events, including DNA packaging and chromatin remodeling. pSILAC offers a comprehensive evaluation of protein synthesis dynamics that are operative during HIV-1 infection. The data serves also to validate studies performed in past decades, while shedding light onto unexplored areas of cellular responses to progressive HIV-1 infection.

EXPERIMENTAL PROCEDURES

Cell Culture and Viral Infection

Primary human monocytes were obtained through leukophoresis of donors that were seronegative for HIV-1, HIV-2, and hepatitis and were purified by countercurrent centrifugal elutriation.[18] Cells were plated in Dulbecco's Modified Eagle's Media supplemented with 10% human serum, 2 mM L-glutamine, 2 μg/mL macrophage colony stimulating factor (MCSF, a generous gift from Pfizer Inc., Cambridge, MA), 10 μg/mL ciprofloxacin and 50 μg/mL gentamicin (complete media). Three million cells/well were plated in 6 well plates at a density of one million cells/mL. Half of the media was exchanged every other day. At day seven, media was removed and cells infected with the HIV-1_{ADA} strain at a multiplicity of infection (MOI) of 0.1 infectious viral particles per cell. Productive HIV-1 infection was monitored by reverse transcriptase (RT) activity in culture supernatant fluids collected on days 3, 5, and 7 following HIV-1 infection (data not shown).

Addition of SILAC Medium

SILAC medium was prepared using two different combinations of isotopically labeled L-Arginine and L-Lysine: "Medium" complete macrophage media, where L-Arginine and L-Lysine were replaced with [$^{13}C_6$]-L-Arginine and [D_4]-L-Lysine (SIGMA-Isotec, St Louis, MO), and "Heavy" complete macrophage media, where L-Arginine and L-Lysine were replaced with [$^{13}C_6$, $^{15}N_4$]-L-Arginine and [$^{13}C_6$, $^{15}N_2$]-L-Lysine (SIGMA-Isotec, St Louis, MO).[12] SILAC media without MCSF was added on days 1, 3, or 5 following HIV-1 infection and cells lysed 48 h following SILAC medium addition. "Medium" macrophage media was applied to uninfected control cells and "Heavy" was applied to infected cells (Figure 1). This was repeated with three independent donors.

Cell Lysis and Sample Preparation

After 48 h incubation in SILAC media, all media was removed, cells were washed with PBS and lysed in lysis buffer (4% sodium dodecyl sulfate, 0.1 M dithiothreitol, 0.1 M Tris-HCl, pH 7.6); cells scraped and collected; and lysates boiled. Protein concentrations of the lysates were determined by Pierce 660 Assay (Thermo Fisher Scientific, Rockford, IL) At each sample day, 50 μg of protein from infected cells were combined with 50 μg of protein from uninfected control cells. Combined lysates were diluted in UA (8 M Urea, 0.1 M Tris-Hcl, pH 8.5), applied to a 30 kDa molecular weight cutoff centrifugal filter (Millipore, Bellerica, MA), and centrifuged at 14 000× *g* for 15 min. Lysates were washed with UA and centrifugation was repeated. IAA (0.5 M iodoacetamide) was added to the filter, incubated at room temperature, and the filter centrifuged at 14 000× *g* for 10 min. The filter unit was washed with UA, and centrifugation was repeated. ABC (0.05 M NH_4HCO_3) was added to the filter, centrifuged, and repeated once. Two micrograms of trypsin (Promega, Madison, WI) in ABC was applied to the filter, mixed for 1 min, and incubated for 18 h at 37 °C in a humidified chamber. The filter-containing digested peptides was transferred to a new collection tube and centrifuged at 14 000× *g* for 10 min. The filter was washed with 0.5 M NaCl and centrifuged at 14 000× *g* for 10 min [adapted from ref 19]. The digested sample was brought to 1 mL total volume with 0.2% formic acid. The acidified protein was added to a wet MXC 30 mg extraction cartridge (Waters-Oasis, Milford, MA) in 1 mL 50% methanol, and the cartridge was washed with 1 mL of 5% methanol/0.1% formic acid, then 100% methanol. The proteins were eluted with 1 mL elution buffer (1.4% NH_3OH in methanol) and dried using a SpeedVac.

Isoelectric Focusing/Fractionation and Mass Spectrometry Sample Preparations

Dried samples were resuspended and separated by isoelectric focusing through OFFGEL electrophoresis (Agilent, Santa Clara, CA) following the manufacturer's suggested protocol for separating peptides.[20] Samples were separated on a pH 3−10 strip and collected into 12 wells. Wells were washed with 200 μL 50% methanol/1% formic acid. Wash was collected, dried in a SpeedVac, and previously collected samples from the corresponding wells were combined with the dried wash.[21] Fractions collected from OFFGEL electrophoresis were mixed 3 parts sample to 1 part 2% trifluoroacetic acid (TFA) and 20% acetonitrile (ACN). C18 spin columns (Thermo Fisher, Rockford, IL) were placed in collection tubes and activated by the addition 100% ACN, followed by being washed with 0.5% TFA and 5% ACN. Diluted samples were applied to the prewet column twice and washed with 0.5% TFA and 5% ACN. The column was placed in a new

dx.doi.org/10.1021/pr200124j |*J. Proteome Res.* 2011, 10, 2852–2862

receiver tube, and peptides were eluted with the addition of 70% ACN. Samples were dried using a SpeedVac and resuspended in 6 μL 0.1% formic acid for LC−MS/MS analysis.

Mass Spectrometry

An LTQ Orbitrap XL with Eksigent nano-LC system was used, equipped with two alternating peptide traps and a PicoFrit C18 column-emitter (New Objective, Woburn, MA). Samples were loaded onto the peptide trap with 98:2 HPLC water with 1% formic acid: ACN with 1% formic acid and eluted using a 60 min linear gradient of 0−60% ACN with 1% formic acid. The instrument was tuned using direct infusion of angiotension and calibrated every 2−3 days using standards provided by the manufacturer with Lock Mass. The acquisition method was created in data-dependent mode with one precursor scan in the Orbitrap, followed by fragmentation of the 5 most abundant peaks in the CID, detected in the LTQ. Resolution of the precursor scan was set to 60 000, scanning from 300 to 2000 m/z. Precursor peaks were dynamically excluded after two selections for 60 s. No charge state rejection was used, but previously detected background peaks were included in a mass rejection list. Collision energy was set to 35 using an isolation width of 2 and an activation Q of 0.250.

Quantification and Identification

Files obtained from LTQ-Orbitrap were submitted to MaxQuant (version 1.0.13.8) for peak list generation. The peak list files were searched using Mascot (Matrix Science, Boston, MA) against the International Protein Index (IPI) human database for protein identifications. The search parameters were set as 2 maximum missed cleavages; Carbamidomethyl (C) as fixed modification; *N*-acetyl (Protein) and Oxidation (M) as variable modifications; top 6 MS/MS peaks per 100 Da; and MS/MS mass tolerance of 0.5 Da. Output files from Mascot were submitted back to MaxQuant for final identifications and validation. MaxQuant was used because of its abilities to provide quantitative analysis of large mass spectrometric data sets acquired when performing pSILAC for high-resolution peptide pair detection. Different mass measurements were corrected for achieving mass accuracy. One unique peptide with a minimum length of 6 amino acids was required. A false discovery rate of 0.01 was applied for both protein and peptide identification, ensuring that at most only 1% of proteins would be falsely identified. Ratios were obtained for HIV-1-infected ("Heavy") MDM to Uninfected ("Medium") MDM comparisons for days 3, 5, and 7 following infection. Significant protein ratio cutoff was set at a Significance B value $\leq$0.05 as calculated by MaxQuant.[22,23] Since proteins of high abundance have high-intense signals and can be measured more accurately than ones with low abundance, we used the B-value because it groups the proteins of similar intensities into bins of equal occupancy and estimates the standard deviation of the protein ratios using the protein subset grouped into the same intensity bin. Contaminants and reverse hits identified by MaxQuant were excluded from further analysis. Heatmap was generated using pretty heatmap package in R.[24] Expression pathways were created using Ingenuity Pathway Analysis (IPA, Ingenuity Systems, Inc., Redwood City, CA) version 8.8.

Bioinformatic Analyses

The proteins that were determined significant by MaxQuant analyses were analyzed with functional profiling tools. A two-step approach was used where significantly differentially expressed proteins were first selected. For bioinformatic analyses, official gene names corresponding to the proteins identified were determined using an internal computational tool. This tool cross-references databases from ENSEMBL and NCBI (our unpublished work). To obtain gene lists for proteins present uniquely or commonly among the three time points, the intersection of genes was determined computationally. Insights into biological processes were investigated by FatiGO,[25] which uses Gene Ontology (GO)[26] and Kyoto Encyclopedia of Genes and Genomes (KEGG)[27] for functional annotations. This extended the search for biological interpretations of the data set to other databases such as the Reactome and Interpro. Functional significance of data collected was measured by Fisher's exact test using 2 $\times$ 2 contingency tables. A low p-value of 0.05 indicated a significant association, and the adjusted p-values were calculated using the false discovery rate (FDR) method.[28]

In creating gene lists, an imposition of threshold was performed. The data was analyzed as described, or correlation analyses were used. The threshold-based method ignores the cooperative behavior among genes, while the correlation analysis incorporates this property. Using the threshold-based method, we obtained a total of 297 unique and 57 common genes that were included in the functional enrichment study. Using the MaxQuant generated $\log_2$(H/M) values from the three experimental time points, gene-to-gene Pearson's correlation coefficients were calculated. A network of highly correlated genes (>95%) was used in the construction of a graph network. The gene network topology was analyzed using Cytoscape 2.6.3,[29] and the densely correlated gene clusters were identified using MCODE V1.2[30] available as a plug-in for Cytoscape.

HIV-1p24 Immunohistochemistry

Monocytes were plated at a density of 10^6 cells/mL, propagated in complete media, infected with virus (MOI of 0.1), and then stained for HIV-1p24 proteins. Briefly, cells were fixed in 4% paraformaldehyde, permeabilized with 1% Triton X-100, washed in PBS, and blocked with 10% bovine serum albumin. HIV-1p24 Ab (Santa Cruz Biotechnology, Santa Cruz, CA) was used at a 1:100 dilution in 10% BSA according to established protocols.[31]

RESULTS AND DISCUSSION

MP display a range of functional innate immune activities for host survival and homeostasis, including: clearance of debris, intracellular destruction of pathogens, and secretion and presentation of bioactive chemicals and peptides that help orchestrate an immune response. In addition, the same cells serve as primary targets for a variety of microbial pathogens, including HIV-1. Indeed, MP support productive HIV-1 infection and are impacted, in structure and function, by both viral and cellular products serving to sustain or restrict the viral life cycle.[32] Virus infection of MP induces a plethora of intracellular activities that affect antiretroviral immunity but fail, collectively, to eliminate the viral pathogen. The mechanism(s) by which this occurs remains incompletely understood. While studies have been performed to elucidate the host proteins required for HIV-1 infection,[33] little was done to elucidate dynamic host protein expression during the course of infection in primary macrophages. Thus, to better determine the consequences of virus-macrophage interactions, we employed pSILAC to examine differential protein expression during the course of infection. This approach is novel, as it allows examination of *de novo* protein synthesis, and as such, is reflective of viral−host cell dynamics.

To link viral replication to protein identifications, we stained infected cells for HIV-1p24 to document the course of HIV-1_{ADA} infection at the time points examined by proteomics. The percentages of infected cells increased over time and are illustrated in Figure 2. On days 3, 5 and 7, 17.6 ± 3.7, 44.0 ± 9.1 and 70.7 ± 4.4% of the MDM were HIV-1p24 positive, respectively. HIV-1_{ADA} MDM infection levels correlated with the formation of multinucleated giant cells (Figure 2); a stage of infection when cell death is not prominent.[18] It is understood that cell death can result after long-standing infection (2 weeks or longer). This occurs, in part, due to laboratory adaptation of the HIV-1_{ADA} strain used in study. Virus-induced macrophage death is not typical of either primary HIV-1 isolates or with the this current strain when MDM are infected for one week at an MOI of 0.1.

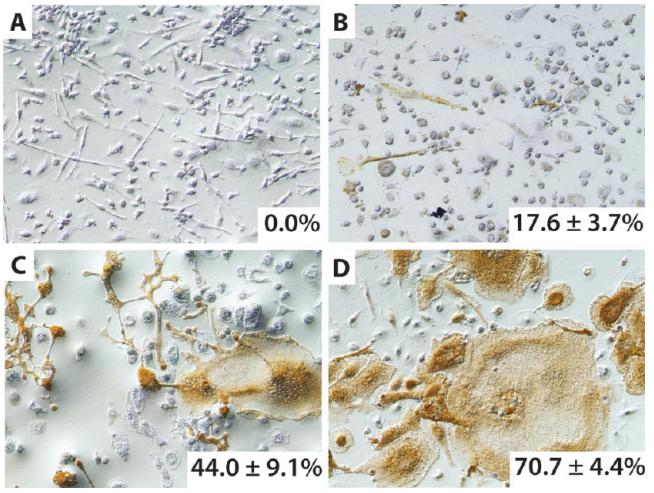

Figure 2. MDM immunostained for HIV-1p24 protein expression calculated as percent of HIV-1p24 positive cells, expressed as ±1 standard deviation of the mean. Illustrated are (A) control, uninfected MDM and HIV-1-infected MDM on (B) day 3, (C) day 5, and (D) day 7 after viral infection.

A total of 393 proteins were identified as differentially expressed, with significance values of ≤0.05 for at least one of the 3 time points examined after HIV-1 infection (Figure 3a). At all time points, 28 proteins were identified as differentially expressed. The number of proteins that were identified between only two of the time points were similar in quantity, no matter which overlapping days were examined. Thirty-two, 28, and 24 common proteins with significant ratios between infected and uninfected MDM were observed on days 3 and 5, 5 and 7, or 3 and 7 after infection, respectively. The numbers of unique proteins with differentially expressed synthesis rates at single time points were 99, 77, and 105 on days 3, 5, and 7 after

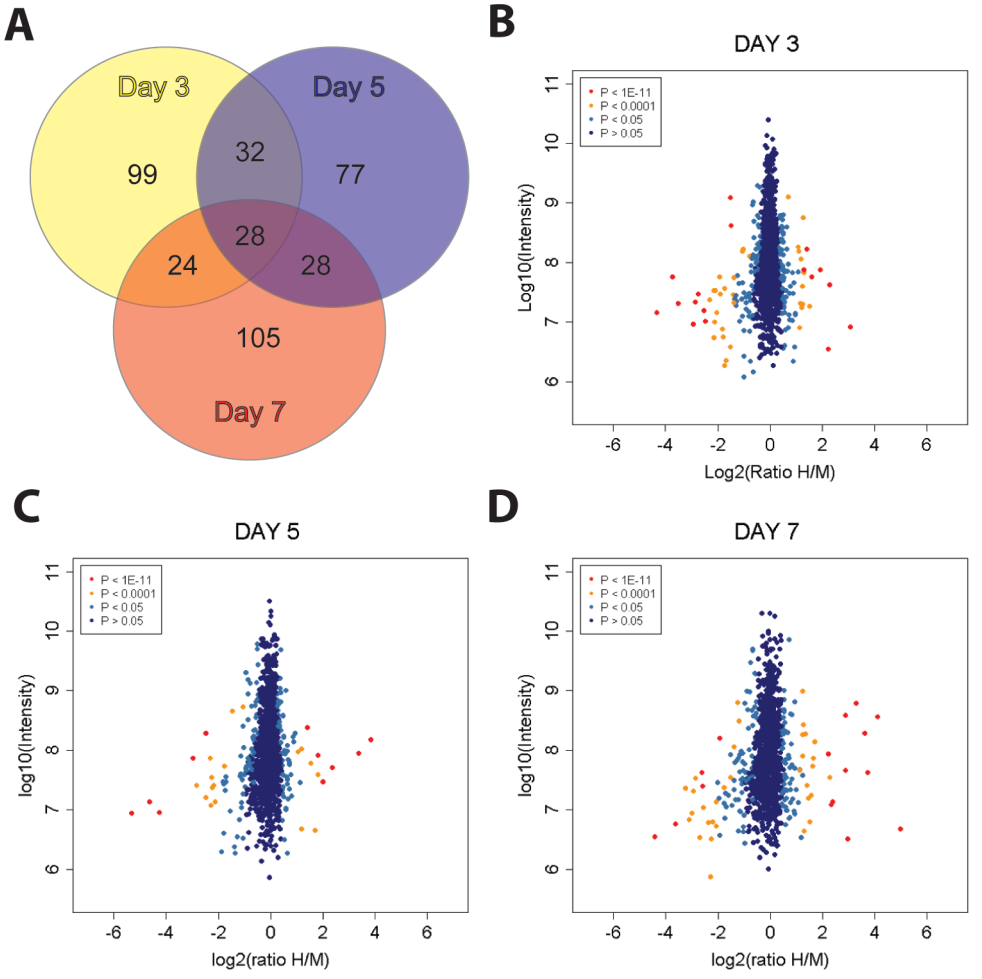

Figure 3. (A) Venn diagram of the overlap in protein identification with significant ratios (Significance B ≤ 0.05) between days 3, 5, and 7. Distribution of $\log_2$ transformed protein expression ratios of HIV-1 to control on (B) day 3, (C) day 5, and (D) day 7 post HIV-1 infection. Ratios are graphed versus intensity.

dx.doi.org/10.1021/pr200124j |J. Proteome Res. 2011, 10, 2852–2862

infection, respectively. These differences demonstrate that the cellular response to HIV-1 infection change during the course of viral infection.

pSILAC ratios were obtained comparing the levels of newly synthesized proteins in HIV-1-infected MDM to their time-matched uninfected controls. On each day, there were proteins with significantly different ratios, as indicated by B values ≤ 0.05, and with changes (up or down regulation) in rates of new protein synthesis between HIV-1 infected cells and replicate uninfected controls (Figure 3b−d). While differentially expressed proteins showed similar findings, their distribution was not constant during the course of viral infection (Figure 3a). Indeed, MDM protein levels in response to HIV-1 infection was altered as viral infection progressed, reflecting time-dependent variances in protein expression rates.

A complete list of all significant proteins and their corresponding fold change are included in Supplemental Table 1 (Supporting Information). The highest scoring interaction network identified by IPA for day 7 of infection identified significant upregulation in *de novo* synthesis of IFN-induced proteins (Figure 4), therefore, indicating that the rate of antiviral response by the macrophage increased as HIV-1 infection progressed. These antiviral proteins affect different points during the viral life cycle (Supplemental Figure 1, Supporting Information). Although numerous antiviral proteins were up-regulated [including: 2′-5′-oligadenylate sythetase 2 (2−5 OAS2), signal transducers and activators of transcription 1 (STAT1), IFN-induced guanylate-binding protein 1 and 2 (GBP1, GBP2), IFN-induced GTP-binding protein Mx1 (Mx1), and bone marrow stromal antigen 2 (BST2 or tetherin)], virus production increased over time, therefore allowing cells to secrete progeny virus or to spread infection to nearby cells (Supplemental Figure 1). While it is known that MCSF-differentiated macrophages display an M2 anti-inflammatory phenotype,[34] it is known that HIV-1 induces an M1 inflammatory phenotype at early stages of infection.[6] This commonly results in IFN production and secretion of pro-inflammatory factors[5,35] demonstrating innate antiretroviral responses of MDM.

STAT1 was upregulated at all 3 time points that were examined at 2-day intervals after infection. STAT1 is known to be an IFN-induced transcription factor (Supplemental Figure 1, Supporting Information). Its expression leads to the induction of downstream antiviral genes, such as 2−5 OAS and tetherin,[36] both of which had increased rates of synthesis. Interestingly, others found that IFN-induction of STAT1 can lead to an initial phosphorylation of STAT1, but a prolonged upregulation of unphosphorylated STAT1 can induce antiviral gene expression independent of STAT1 phosphorylation.[36] This could explain the increased and prolonged rates of synthesis of new STAT1 identified in our study, which translates to upregulation of antiviral genes and further substantiating that MDM employ multiple mechanisms to clear virus and permit host cell survival.

Tetherin binds budding HIV-1 virions to the cell membrane, and thus inhibits their release. Viral protein U (Vpu) can inhibit tetherin expression by binding tetherin at the membrane leading to down-regulation of tetherin at the cell surface[37] (Supplemental Figure 1, Supporting Information). Tetherin not only inhibits virion release, but also cell-to-cell viral transfer.[38] We saw an initial down-regulation of tetherin synthesis on D3 that transitions to up-regulation on D5 and progressing even further by D7. This increase in the synthesis rate may be an effort to bypass Vpu inhibition in a futile attempt to control viral propagation. Another IFN-induced antiviral protein, 2−5 OAS2, exhibited an increased rate of synthesis in our study was shown to be elevated in individuals afflicted with acquired immune deficiency syndrome (AIDS) compared with uninfected controls.[39] In simian immunodeficiency virus models, 2−5 OAS2 expression is elevated in those subjects with a more rapid progression toward AIDS.[40] HIV-1 is known to have mechanisms to evade the interferon-induced effects of 2−5 OAS2.[41] Tat binding to the transactivation responsive region of HIV-1 mRNA blocks 2−5 OAS2 binding, therefore preventing 2−5 OAS2 activation.[42] While we have identified an increasing rate of 2−5 OAS2 synthesis as HIV-1 infection progresses, viral infection is not diminished as demonstrated by both HIV-1p24 staining and RT activity. Mx1 and GBP (Supplemental Figure 1) both have roles in the inhibition of hepatitis C.[43,44] Mx1 also has been implicated in inhibiting influenza viral growth,[45] and GBP is known to inhibit both vesicular stomatitis and encephalomyocarditis viruses.[46] MX1 induction during HIV-1 infection has been identified by multiple groups.[47] Thus, extensive identification of IFN-induced antiviral proteins that have increased synthesis during HIV-1 infection confirms pSILAC as a suitable technology for detecting protein synthesis changes in nondividing MDM.

ENSEMBL Gene Identifiers for corresponding proteins within a group were obtained for functional classification of identified proteins. The number of unique genes identified for the three days are listed in Table 1 and were further analyzed for functional classification. To begin looking for novel protein synthesis changes that occurred during HIV-1 infection of MDM and were identified by pSILAC, corresponding genes were grouped by their functional classification using FatiGO, a functional enrichment tool available in the Babelomics software. Only groupings of genes scoring a p-value ≤ 0.01 were considered significant and used for further analyses. We examined GO terms that contained significant groupings of unique proteins identified in a minimum of two time points. To this end, a significant number of protein groups on each of the days corresponded to one GO term, but the individual proteins identified between days were unique. Such analyses bridged the data set to functional biology of the macrophage. In this way, the impact of protein groups with specific functions was realized as significant for virus-infected cells.

Through investigations of new protein synthesis observed during short time periods, we can elucidate an evolving MDM response to HIV-1 infection. Understanding the compensatory changes in MP biology after viral infection is key to identifying both how the cell responds to progressive HIV-1 infection and the mechanisms by which HIV-1 modulates the cellular response to its benefit. In this regard, a number of cellular protein classes changed their rate of synthesis as a consequence of infection. While many groups of proteins were determined to be significantly altered, we chose to focus our attention on the most enriched functional groupings; those grouped under the GO terms: telomere maintenance, chromatin assembly or disassembly, DNA packaging, and nucleosome assembly. Each of these groups is marked with an asterisk in Table 2 and had a minimum of 15 unique genes associated with D7 or D3 along with separate unique genes associated with all three days of infection. While telomere maintenance was identified as an enriched grouping, these proteins were all histones, known to be involved in cellular regulatory processes. Proteins linked only to the maintenance of telomeres were not identified and would be expected since human MDM are nondividing cells. The groupings related to

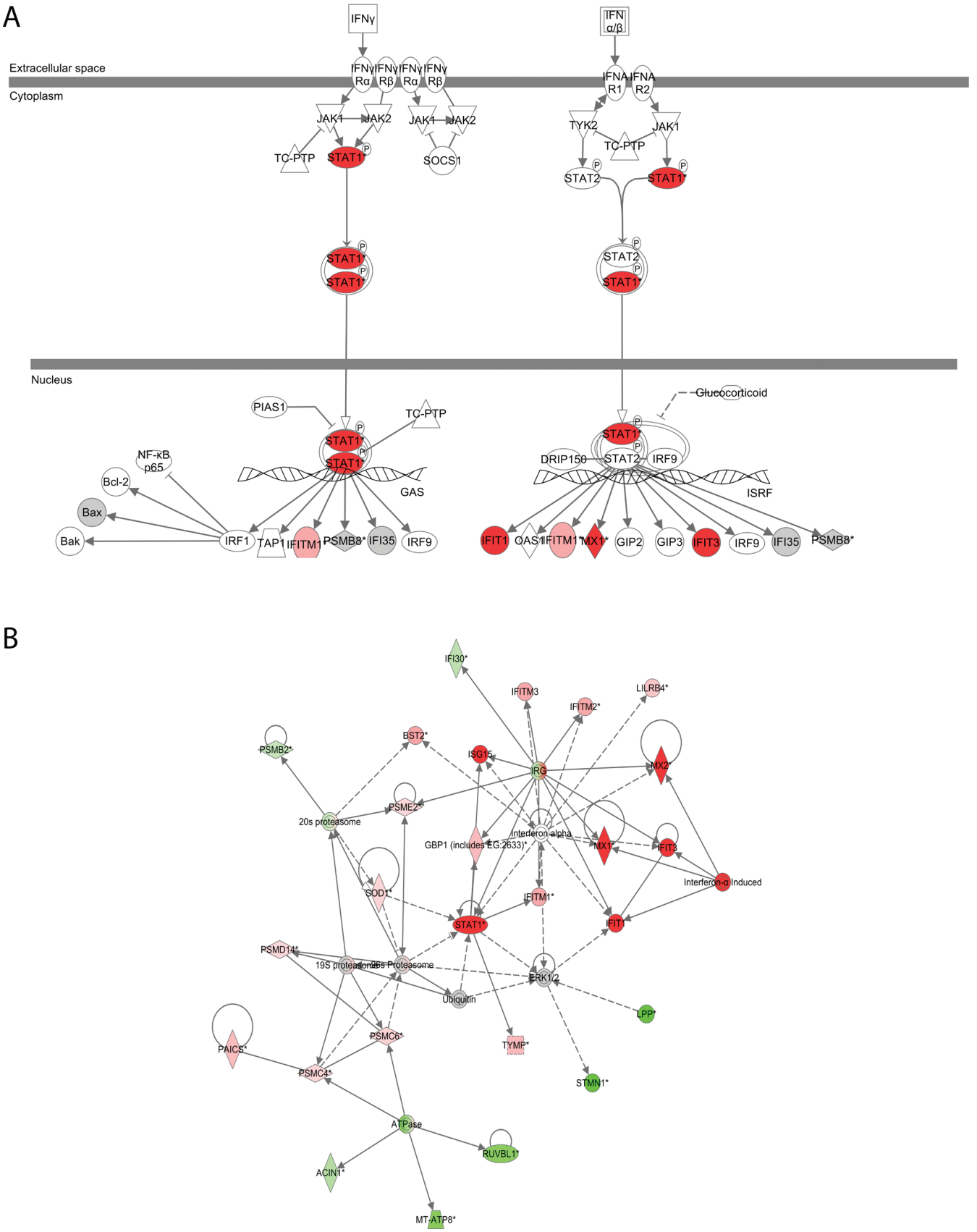

Figure 4. (A) IFN signaling pathway coded with identified proteins on day 7 postinfection. Gray proteins were identified but did not reach statistical significance. (B) Ingenuity Pathway Analysis highest scoring interaction network. Increased synthesis rates are indicated by increasing intensity of red; decreased synthesis rates are denoted in green.

dx.doi.org/10.1021/pr200124j |*J. Proteome Res.* 2011, 10, 2852–2862

the control of DNA packaging and chromatin assembly are likely linked to virus-induced cytopathology, which is highly significant for the HIV-1_{ADA} strain.

MaxQuant protein groups were also examined in parallel for interactions between one another and to provide confirmation and extensions of the protein maps. Indeed, by performing cluster analysis, we selected two clusters that included interactions from highly significant groupings that are linked to macrophage functions. The first cluster demonstrates specific interactions between DNA packaging, chromatin assembly/disassembly, and nucleosome assembly, along with fatty acid oxidation and antigen processing and presentation (Figure 5, Supplemental Figure 2, Supporting Information). In the second cluster, we identified interactions that appeared to split between two distinct groups (Supplemental Figures 3 and 4, Supporting Information). The first was between transcription initiation, nucleosome assembly, chromatin assembly/disassembly, DNA packaging, second messenger signaling and phosphoinositide-mediated signaling. The second was involved in the immune system and developmental regulation, including negative regulation of cellular differentiation, regulation of immune system processes, myeloid cell differentiation, megakaryocyte differentiation, hemopoiesis, and immune system development. A third, but less significant, contributor was the regulation of ubiquitin-protein ligase activity (both positive and negative).

The cytopathology of HIV-1 infected MDM has been the topic of previous studies investigating cytoskeletal transformation, multinucleated giant cell formation, and HIV-1-associated neurodegeneration.[8,35] Less studied are the protein changes resulting in these cytopathological findings. The epigenetic control of HIV-1 viral latency has been the subject of many recent studies and helps to explain the cytopathicity of HIV-1 infection. While histone methylation, acetylation and deacetylation are utilized to control viral integration and expression,[48] histone synthesis and turnover is an area that has not been heavily investigated in relation to HIV-1 infection. We identified differential regulation in the synthesis rates of histone proteins, which are seen in our significant GO groupings (Figure 6). Significant down-regulation in synthesis rates were identified in some histones by D3 post infection, and further down-regulation in the rates of protein synthesis were identified by days 5 and 7 following infection. Such a response is made when the host cell works to restrict viral dissemination in MDM. Indeed, histone recycling during transcription is thought to occur when it is necessary to replace modified histones, such as those that are methylated.[49]

In recent years, it has been determined that modified histones are often controlled by such molecules as histone methyltransferases, acetyltransferases, and deacetylases, without the need for histone recycling. In contrast, histone replacement from cellular pools is necessary following unwinding during transcription, substantiating the need for histone turnover for active transcription.[50] HIV-1 infection results in chromatin disruption, which likely contributes to the accessibility of transcription initiation sites to polymerases in productively infected cells.[51] Therefore, it is required to rearrange DNA packaging for successful proviral DNA insertion and subsequent transcription. While the location and modification status of histones commonly have been examined,[52] along with other mechanisms of epigenetic control of viral replication,[53] the rate of new histone synthesis has not been evaluated as a consequence of HIV-1 infection. Indeed, decreasing synthesis rates of macrophage histone proteins may therefore serve a dual function in altering

Table 1. Number of Unique Genes Used for Babelomics Functional Annotation Following Parsing of Original Significant MaxQuant Protein Groupings

treatment	significant MaxQuant proteins	ENSEMBLE gene identifiers	unique genes
Day 3	184	221	98
Day 5	165	201	76
Day 7	186	248	123

Table 2. Functional Annotation of Genes Using Babelomics[a]

GO Terms	knowledgebase used	number of unique genes			
		day 3	day 5	day 7	common (day 3, 5, 7)
3′ -UTR-mediated translational regulation	Reactome		4	4	
APC/C:Cdh1-mediated degradation of Skp2	Reactome	3		5	
Cdc20:Phospho-APC/C mediated degradation of Cyclin A	Reactome	3		5	
Cell cycle, Mitotic	Reactome	7		7	
Diabetes pathways	Reactome	7		7	
DNA replication	Reactome	4		5	
Gene expression	Reactome	7		8	
HIV infection	Reactome	4		7	
Metabolism of amino acids	Reactome	5		7	
Regulation of activated PAK-2p34 by proteasome mediated degradation	Reactome	3		5	
Signaling by Wnt	Reactome	3		5	
Telomere Maintenance*	Reactome			15	8
Fatty acid metabolism	Kegg Pathway	4		4	
Proteasome	Kegg Pathway	3		5	
Chromatin assembly or disassembly*	Biological Process			20	27
DNA packaging*	Biological Process			21	27
Nucleosome assembly*	Biological Process			18	27

[a] Numbers in each column correspond to the number of unique genes expressed only at that day.

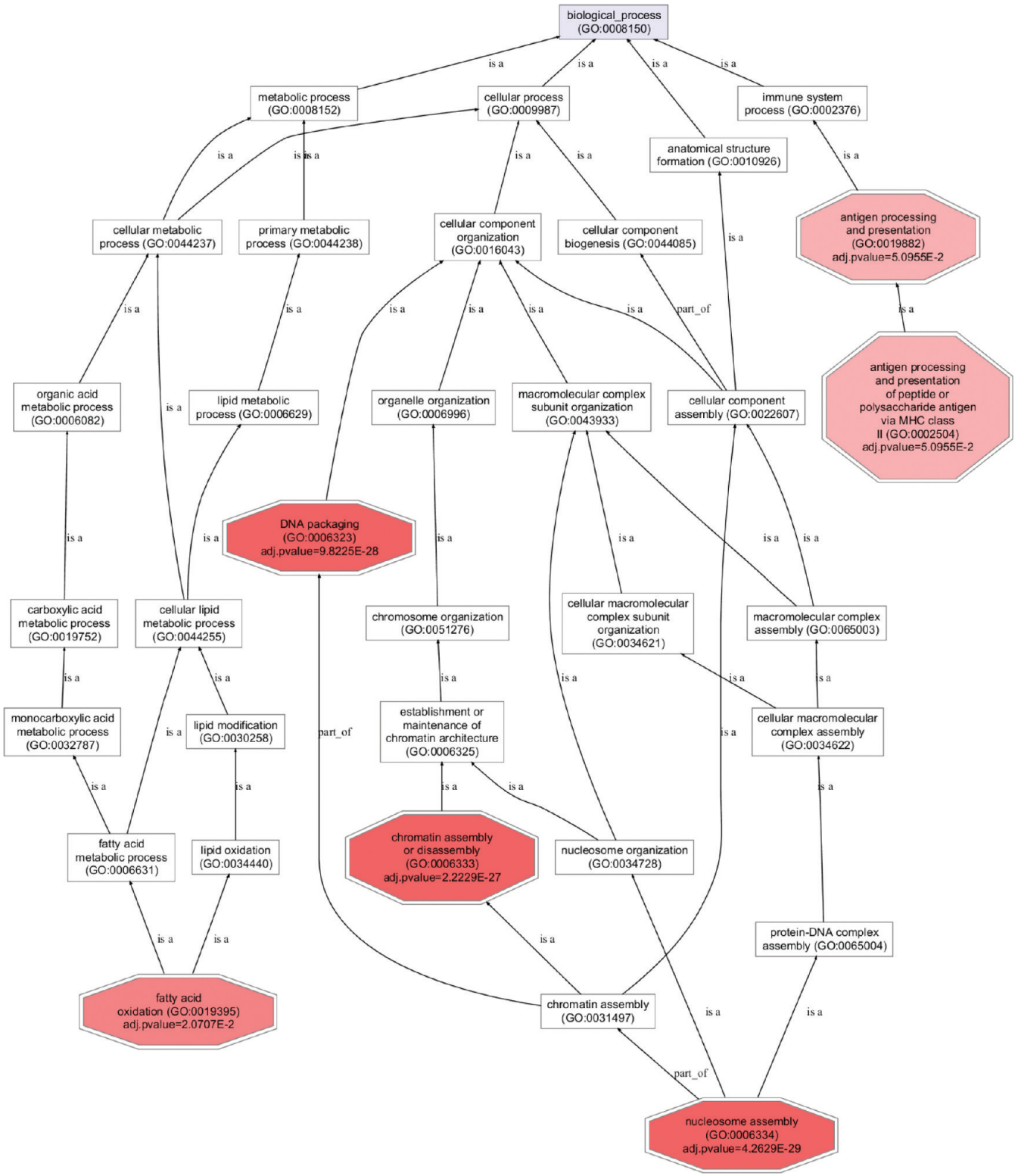

Figure 5. Enriched protein classifications for the correlation network in Supplemental Figure 2 (Supporting Information).

cellular structure and metabolism. First, it may permit improved engagement of the HIV-1 promoter to facilitate active viral replication, and second, an overall decrease in transcription, or rearrangement of chromatin, can effect more globally altered gene expression as the host works to protect the cell from ongoing virus-induced damage.

The findings also support the idea that the macrophage has an initial burst in protein synthesis rates required for antigen (AG) presentation to both CD4+ and CD8+ T cells as an attempt to control viral infection. This response is likely attenuated over time as the mechanism by which macrophages work to clear virus and protect the host, shifts and begins to break down.

dx.doi.org/10.1021/pr200124j |J. Proteome Res. 2011, 10, 2852–2862

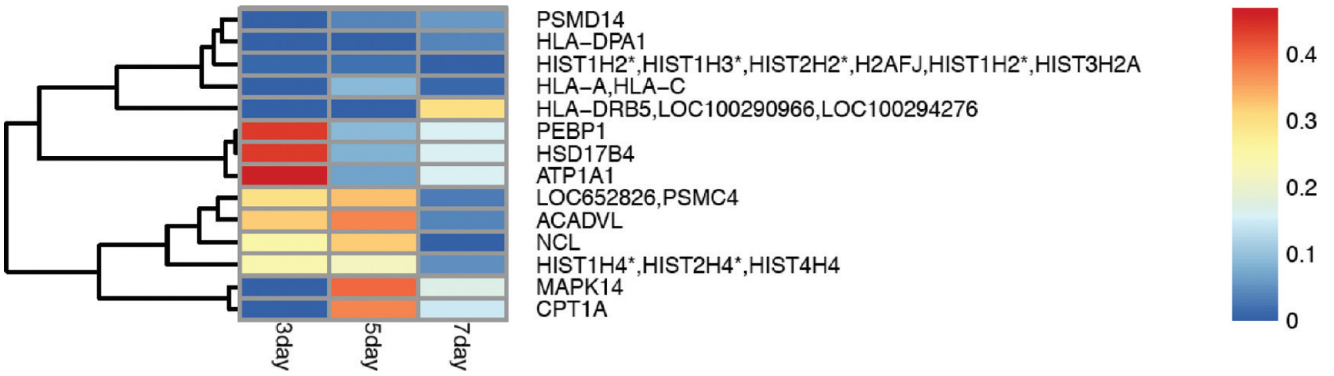

Figure 6. Heatmap of $\log_2$ (H/M ratio) labeled by their gene name. Expression between days 3, 5, and 7 is colored with varying intensities ranging from blue to red; blue being the lowest ratio, red being the highest ratio, and yellow representing those ratios that equal one.

Interestingly, the AG presentation protein group includes a variety of major histocompatibility complex (MHC) class I and MHC class II proteins. Its synthesis was most heavily upregulated at day 3 compared with the later days, 5 and 7, of infection (Figure 6). As virus replication progressed, AG presentation-related protein synthesis rates consistently increased compared to controls; but the level of upregulation was decreased over time. It is noteworthy that AG presentation to T cells is a major function of macrophages and represents, along with phagocytosis, intracellular killing, mobility, and secretion of bioactive substances, the host's primary defense in engaging an immune response to contain microbial infection. Thus, up-regulation in both, MCH Class I and II AG presenting proteins that are reduced as HIV-1 infection ensues, likely follows a cellular response to control this ongoing microbial infection. During early infection, before large increases in viral replication overwhelms cellular control capacities, the macrophage attempts to control virus through its AG presentation capabilities. In support of this notion, and recently seen by others, Nef was implicated in both MHC I[54] and MHC II[55] down-regulation, further substantiating that HIV-1 modulates the macrophage to its benefit. Indeed, we found that as HIV-1 infection progresses, AG presentation activities are diminished. This can be due to a combination of cellular responses including Nef inhibition and modulation of macrophage protein expression leading to enhanced cell survival.

CONCLUSION

Taken together our data support the idea that a delicate interplay exists between host survival and macrophage viral propagation. While ultimately HIV-1 persistence prevails, intricate cellular and viral regulatory events occur as the macrophage works to contain HIV-1 infection, despite the inevitable outcome to the cell. HIV-1 in turn acquires unique protective mechanisms to support its own survival, while altering the MDM to its benefit. Indeed, our study highlights a range of antiretroviral mechanisms that develop in the macrophage for its benefit. Down-regulation of histone synthesis rates is one that portends more global outcomes for the cell. Altering DNA packaging ultimately alters transcription rates and cell process regulation. Ultimately, HIV-1 overcomes the antiretroviral macrophage protein armada. While working to contain viral growth, the macrophage fails, inevitably giving the virus and its dissemination the overriding edge. The future rests in finding the means to boost macrophage antiretroviral activities with the goal to both contain, then eliminate viral infection.

ASSOCIATED CONTENT

Supporting Information

Supplemental tables and figures. This material is available free of charge via the Internet at http://pubs.acs.org.

AUTHOR INFORMATION

Corresponding Author

*Howard E. Gendelman, MD, Department of Pharmacology and Experimental Neuroscience, University of Nebraska Medical Center, 985800 Nebraska Medical Center, Omaha, NE 68198-5880. Phone: 402 559 8920. Fax: 402 559 3744. E-mail: hegendel@unmc.edu.

ACKNOWLEDGMENT

We thank Ms. Melinda Wojtkiewicz and the mass spectrometry and proteomics core facility at the University of Nebraska Medical Center for assistance in running samples; Ms. Rufina Dominic Savio for her assistance in running MaxQuant; Mr. Landon Ehlers for his contribution to the viral detection; Dr. R. Lee Mosley for critical reading of the manuscript; and Dr. Fang Yu's assistance in MaxQuant data interpretation. This work was supported in part by the Carol Swarts MD Neuroscience Research Laboratory and National Institutes of Health grants: P01 DA028555, R01 NS36126, P01 NS31492, 2R01 NS034239, P20 RR15635, P01 MH64570, and P01 NS31492 (H.E.G.); P30 MH062261 and R01 DA03096 (H.F.); P01 NS43985 (H.E.G. and P.C.); and P01 DA026146 (H.F., H.E.G. and P.C.).

REFERENCES

(1) Ciborowski, P.; Gendelman, H. E. Human immunodeficiency virus-mononuclear phagocyte interactions: emerging avenues of biomarker discovery, modes of viral persistence and disease pathogenesis. *Curr. HIV Res.* **2006**, *4* (3), 279–91.

(2) Cassol, E.; Alfano, M.; Biswas, P.; Poli, G. Monocyte-derived macrophages and myeloid cell lines as targets of HIV-1 replication and persistence. *J. Leukoc. Biol.* **2006**, *80* (5), 1018–30.

(3) Le Douce, V.; Herbein, G.; Rohr, O.; Schwartz, C. Molecular mechanisms of HIV-1 persistence in the monocyte-macrophage lineage. *Retrovirology* **2010**, *7*, 32.

(4) Herbein, G.; Gras, G.; Khan, K. A.; Abbas, W. Macrophage signaling in HIV-1 infection. *Retrovirology* **2010**, *7*, 34.

(5) Cassol, E.; Cassetta, L.; Alfano, M.; Poli, G. Macrophage polarization and HIV-1 infection. *J. Leukoc. Biol* **2010**, *87* (4), 599–608.
(6) Herbein, G.; Varin, A. The macrophage in HIV-1 infection: from activation to deactivation? *Retrovirology* **2010**, *7*, 33.
(7) Heinzinger, N.; Baca-Regen, L.; Stevenson, M.; Gendelman, H. E. Efficient synthesis of viral nucleic acids following monocyte infection by HIV-1. *Virology* **1995**, *206* (1), 731–5.
(8) Kadiu, I.; Ricardo-Dukelow, M.; Ciborowski, P.; Gendelman, H. E. Cytoskeletal protein transformation in HIV-1-infected macrophage giant cells. *J. Immunol.* **2007**, *178* (10), 6404–15.
(9) Ong, S. E.; Mann, M. Stable isotope labeling by amino acids in cell culture for quantitative proteomics. *Methods Mol. Biol.* **2007**, *359*, 37–52.
(10) Ong, S. E.; Mann, M. A practical recipe for stable isotope labeling by amino acids in cell culture (SILAC). *Nat. Protoc.* **2006**, *1* (6), 2650–60.
(11) Schwanhausser, B.; Gossen, M.; Dittmar, G.; Selbach, M. Global analysis of cellular protein translation by pulsed SILAC. *Proteomics* **2009**, *9* (1), 205–9.
(12) Selbach, M.; Schwanhausser, B.; Thierfelder, N.; Fang, Z.; Khanin, R.; Rajewsky, N. Widespread changes in protein synthesis induced by microRNAs. *Nature* **2008**, *455* (7209), 58–63.
(13) Du, R.; Long, J.; Yao, J.; Dong, Y.; Yang, X.; Tang, S.; Zuo, S.; He, Y.; Chen, X. Subcellular quantitative proteomics reveals multiple pathway cross-talk that coordinates specific signaling and transcriptional regulation for the early host response to LPS. *J. Proteome Res.* **2010**, *9* (4), 1805–21.
(14) Xue, Y.; Yun, D.; Esmon, A.; Zou, P.; Zuo, S.; Yu, Y.; He, F.; Yang, P.; Chen, X. Proteomic dissection of agonist-specific TLR-mediated inflammatory responses on macrophages at subcellular resolution. *J. Proteome Res.* **2008**, *7* (8), 3180–93.
(15) Gu, S.; Wang, T.; Chen, X. Quantitative proteomic analysis of LPS-induced differential immune response associated with TLR4 Polymorphisms by multiplex amino acid coded mass tagging. *Proteomics* **2008**, *8* (15), 3061–70.
(16) Dhungana, S.; Merrick, B. A.; Tomer, K. B.; Fessler, M. B. Quantitative proteomics analysis of macrophage rafts reveals compartmentalized activation of the proteasome and of proteasome-mediated ERK activation in response to lipopolysaccharide. *Mol. Cell. Proteomics* **2009**, *8* (1), 201–13.
(17) Shui, W.; Gilmore, S. A.; Sheu, L.; Liu, J.; Keasling, J. D.; Bertozzi, C. R. Quantitative proteomic profiling of host-pathogen interactions: the macrophage response to Mycobacterium tuberculosis lipids. *J. Proteome Res.* **2009**, *8* (1), 282–9.
(18) Gendelman, H. E.; Orenstein, J. M.; Martin, M. A.; Ferrua, C.; Mitra, R.; Phipps, T.; Wahl, L. A.; Lane, H. C.; Fauci, A. S.; Burke, D. S.; Efficient isolation and propagation of human immunodeficiency virus on recombinant colony-stimulating factor 1-treated monocytes. *J. Exp. Med.* **1988**, *167* (4), 1428–41.
(19) Wisniewski, J. R.; Zougman, A.; Nagaraj, N.; Mann, M. Universal sample preparation method for proteome analysis. *Nat. Methods* **2009**, *6* (5), 359–62.
(20) Horth, P.; Miller, C. A.; Preckel, T.; Wenz, C. Efficient fractionation and improved protein identification by peptide OFFGEL electrophoresis. *Mol. Cell. Proteomics* **2006**, *5* (10), 1968–74.
(21) Ernoult, E.; Gamelin, E.; Guette, C. Improved proteome coverage by using iTRAQ labelling and peptide OFFGEL fractionation. *Proteome Sci.* **2008**, *6*, 27.
(22) Cox, J.; Matic, I.; Hilger, M.; Nagaraj, N.; Selbach, M.; Olsen, J. V.; Mann, M. A practical guide to the MaxQuant computational platform for SILAC-based quantitative proteomics. *Nat. Protoc.* **2009**, *4* (5), 698–705.
(23) Cox, J.; Mann, M. MaxQuant enables high peptide identification rates, individualized p.p.b.-range mass accuracies and proteome-wide protein quantification. *Nat. Biotechnol.* **2008**, *26* (12), 1367–72.
(24) Kolde, R. *Pretty Heatmaps*. http://cran.r-project.org/web/packages/pheatmap/pheatmap.pdf; Last accessed .
(25) Medina, I.; Carbonell, J.; Pulido, L.; Madeira, S. C.; Goetz, S.; Conesa, A.; Tarraga, J.; Pascual-Montano, A.; Nogales-Cadenas, R.; Santoyo, J.; Garcia, F.; Marba, M.; Montaner, D.; Dopazo, J. Babelomics: an integrative platform for the analysis of transcriptomics, proteomics and genomic data with advanced functional profiling. *Nucleic Acids Res.* **2010**, *38* (Suppl), W210–3.
(26) Ashburner, M.; Ball, C. A.; Blake, J. A.; Botstein, D.; Butler, H.; Cherry, J. M.; Davis, A. P.; Dolinski, K.; Dwight, S. S.; Eppig, J. T.; Harris, M. A.; Hill, D. P.; Issel-Tarver, L.; Kasarskis, A.; Lewis, S.; Matese, J. C.; Richardson, J. E.; Ringwald, M.; Rubin, G. M.; Sherlock, G. Gene ontology: tool for the unification of biology. The Gene Ontology Consortium. *Nat. Genet.* **2000**, *25* (1), 25–9.
(27) Kanehisa, M.; Goto, S. KEGG: kyoto encyclopedia of genes and genomes. *Nucleic Acids Res.* **2000**, *28* (1), 27–30.
(28) Benjamini, Y.; Hochberg, Y. Controlling the false discovery rate: a practical and powerful approach to multiple testing. *J. R. Stat. Soc.* **1995**, No. 57, 289–300.
(29) Cline, M. S.; Smoot, M.; Cerami, E.; Kuchinsky, A.; Landys, N.; Workman, C.; Christmas, R.; Avila-Campilo, I.; Creech, M.; Gross, B.; Hanspers, K.; Isserlin, R.; Kelley, R.; Killcoyne, S.; Lotia, S.; Maere, S.; Morris, J.; Ono, K.; Pavlovic, V.; Pico, A. R.; Vailaya, A.; Wang, P. L.; Adler, A.; Conklin, B. R.; Hood, L.; Kuiper, M.; Sander, C.; Schmulevich, I.; Schwikowski, B.; Warner, G. J.; Ideker, T.; Bader, G. D. Integration of biological networks and gene expression data using Cytoscape. *Nat. Protoc.* **2007**, *2* (10), 2366–82.
(30) Bader, G. D.; Hogue, C. W. An automated method for finding molecular complexes in large protein interaction networks. *BMC Bioinform.* **2003**, *4*, 2.
(31) Nowacek, A. S.; Miller, R. L.; McMillan, J.; Kanmogne, G.; Kanmogne, M.; Mosley, R. L.; Ma, Z.; Graham, S.; Chaubal, M.; Werling, J.; Rabinow, B.; Dou, H.; Gendelman, H. E. NanoART synthesis, characterization, uptake, release and toxicology for human monocyte-macrophage drug delivery. *Nanomedicine* **2009**, *4* (8), 903–17.
(32) Stevenson, M.; Gendelman, H. E. Cellular and viral determinants that regulate HIV-1 infection in macrophages. *J. Leukoc. Biol.* **1994**, *56* (3), 278–88.
(33) Brass, A. L.; Dykxhoorn, D. M.; Benita, Y.; Yan, N.; Engelman, A.; Xavier, R. J.; Lieberman, J.; Elledge, S. J. Identification of host proteins required for HIV infection through a functional genomic screen. *Science* **2008**, *319* (5865), 921–6.
(34) Martinez, F. O.; Gordon, S.; Locati, M.; Mantovani, A. Transcriptional profiling of the human monocyte-to-macrophage differentiation and polarization: new molecules and patterns of gene expression. *J. Immunol.* **2006**, *177* (10), 7303–11.
(35) Kraft-Terry, S. D.; Buch, S. J.; Fox, H. S.; Gendelman, H. E. A coat of many colors: neuroimmune crosstalk in human immunodeficiency virus infection. *Neuron* **2009**, *64* (1), 133–45.
(36) Cheon, H.; Stark, G. R. Unphosphorylated STAT1 prolongs the expression of interferon-induced immune regulatory genes. *Proc. Natl. Acad. Sci. U.S.A.* **2009**, *106* (23), 9373–8.
(37) Douglas, J. L.; Gustin, J. K.; Viswanathan, K.; Mansouri, M.; Moses, A. V.; Fruh, K. The great escape: viral strategies to counter BST-2/tetherin. *PLoS Pathog.* **2010**, *6* (5), e1000913.
(38) Casartelli, N.; Sourisseau, M.; Feldmann, J.; Guivel-Benhassine, F.; Mallet, A.; Marcelin, A. G.; Guatelli, J.; Schwartz, O. Tetherin restricts productive HIV-1 cell-to-cell transmission. *PLoS Pathog.* **2010**, *6* (6), e1000955.
(39) Read, S. E.; Williams, B. R.; Coates, R. A.; Evans, W. K.; Fanning, M. M.; Garvey, M. B.; Shepherd, F. A. Elevated levels of interferon-induced 2′-5′ oligoadenylate synthetase in generalized persistent lymphadenopathy and the acquired immunodeficiency syndrome. *J. Infect. Dis.* **1985**, *152* (3), 466–72.
(40) Durudas, A.; Milush, J. M.; Chen, H. L.; Engram, J. C.; Silvestri, G.; Sodora, D. L. Elevated levels of innate immune modulators in lymph nodes and blood are associated with more-rapid disease progression in simian immunodeficiency virus-infected monkeys. *J. Virol.* **2009**, *83* (23), 12229–40.

(41) Bolinger, C.; Boris-Lawrie, K. Mechanisms employed by retroviruses to exploit host factors for translational control of a complicated proteome. *Retrovirology* **2009**, *6*, 8.

(42) Silverman, R. H. Viral encounters with 2′,5′-oligoadenylate synthetase and RNase L during the interferon antiviral response. *J. Virol.* **2007**, *81* (23), 12720–9.

(43) Brodsky, L. I.; Wahed, A. S.; Li, J.; Tavis, J. E.; Tsukahara, T.; Taylor, M. W. A novel unsupervised method to identify genes important in the anti-viral response: application to interferon/ribavirin in hepatitis C patients. *PLoS One* **2007**, *2* (7), e584.

(44) Itsui, Y.; Sakamoto, N.; Kakinuma, S.; Nakagawa, M.; Sekine-Osajima, Y.; Tasaka-Fujita, M.; Nishimura-Sakurai, Y.; Suda, G.; Karakama, Y.; Mishima, K.; Yamamoto, M.; Watanabe, T.; Ueyama, M.; Funaoka, Y.; Azuma, S.; Watanabe, M. Antiviral effects of the interferon-induced protein guanylate binding protein 1 and its interaction with the hepatitis C virus NS5B protein. *Hepatology* **2009**, *50* (6), 1727–37.

(45) Toyoda, T.; Asano, Y.; Ishihama, A. Role of GTPase activity of murine Mx1 protein in nuclear localization and anti-influenza virus activity. *J. Gen. Virol.* **1995**, *76* (Pt 7), 1867–9.

(46) Anderson, S. L.; Carton, J. M.; Lou, J.; Xing, L.; Rubin, B. Y. Interferon-induced guanylate binding protein-1 (GBP-1) mediates an antiviral effect against vesicular stomatitis virus and encephalomyocarditis virus. *Virology* **1999**, *256* (1), 8–14.

(47) Baca, L. M.; Genis, P.; Kalvakolanu, D.; Sen, G.; Meltzer, M. S.; Zhou, A.; Silverman, R.; Gendelman, H. E. Regulation of interferon-alpha-inducible cellular genes in human immunodeficiency virus-infected monocytes. *J. Leukoc. Biol.* **1994**, *55* (3), 299–309.

(48) Hakre, S.; Chavez, L.; Shirakawa, K.; Verdin, E. Epigenetic regulation of HIV latency. *Curr. Opin. HIV AIDS* **2011**, *6* (1), 19–24.

(49) Ehrenhofer-Murray, A. E. Chromatin dynamics at DNA replication, transcription and repair. *Eur. J. Biochem.* **2004**, *271* (12), 2335–49.

(50) Dion, M. F.; Kaplan, T.; Kim, M.; Buratowski, S.; Friedman, N.; Rando, O. J. Dynamics of replication-independent histone turnover in budding yeast. *Science* **2007**, *315* (5817), 1405–8.

(51) Verdin, E.; Paras, P., Jr.; Van Lint, C. Chromatin disruption in the promoter of human immunodeficiency virus type 1 during transcriptional activation. *EMBO J.* **1993**, *12* (8), 3249–59.

(52) Shah, S.; Nonnemacher, M. R.; Pirrone, V.; Wigdahl, B. Innate and adaptive factors regulating human immunodeficiency virus type 1 genomic activation. *J. Neuroimmune Pharmacol.* **2010**, *5* (3), 278–93.

(53) Kilareski, E. M.; Shah, S.; Nonnemacher, M. R.; Wigdahl, B. Regulation of HIV-1 transcription in cells of the monocyte-macrophage lineage. *Retrovirology* **2009**, *6*, 118.

(54) Yi, L.; Rosales, T.; Rose, J. J.; Chowdhury, B.; Knutson, J. R.; Venkatesan, S. HIV-1 Nef binds a subpopulation of MHC-I throughout its trafficking itinerary and downregulates MHC-I by perturbing both anterograde and retrograde trafficking. *J. Biol. Chem.* **2010**.

(55) Chaudhry, A.; Verghese, D. A.; Das, S. R.; Jameel, S.; George, A.; Bal, V.; Mayor, S.; Rath, S. HIV-1 Nef promotes endocytosis of cell surface MHC class II molecules via a constitutive pathway. *J. Immunol.* **2009**, *183* (4), 2415–24.